

Hanna Małuszyńska,* Piotr
Czarnecki, Anna Czarnecka and
Zdzisław Pająk

Physics Department, A. Mickiewicz University,
Umultowska 85, 61-614 Poznań, Poland

Correspondence e-mail: hanmal@amu.edu.pl

Structures and phase transitions in a new ferroelectric – pyridinium chlorochromate – studied by X-ray diffraction, DSC and dielectric methods

Received 4 October 2011

Accepted 9 February 2012

Pyridinium chlorochromate, $[\text{C}_5\text{H}_5\text{NH}]^+[\text{ClCrO}_3]^-$ (hereafter referred to as PyClCrO_3), was studied by X-ray diffraction, differential scanning calorimetry (DSC) and dielectric methods. Studies reveal three reversible phase transitions at 346, 316 and 170 K with the following phase sequence: $R\bar{3}m$ (I) $\rightarrow R3m$ (II) $\rightarrow Cm$ (III) $\rightarrow Cc$ (IV), $c' = 2c$. PyClCrO_3 is the first pyridinium salt in which all four phases have been successfully characterized by a single-crystal X-ray diffraction method. Structural results together with dielectric and calorimetric studies allow the classification of the two intermediate phases (II) and (III) as ferroelectric with the Curie point at 346 K, and the lowest phase (IV) as most probably ferroelectric. The ferroelectric hysteresis loop was observed only in phase (III). The high ionic conductivity hindered its observation in phase (II).

1. Introduction

The search for new molecular ferroelectrics is of special interest because of its potential in the development of electronic and photonic devices (Horiuchi *et al.*, 2005, 2010).

Simple pyridinium salts represent a very interesting group of hybrid organic–inorganic structures in which polymorphic solid–solid phase transitions have been revealed by extensive DSC, NMR, X-ray diffraction and dielectric studies (Hartl, 1975; Hanaya *et al.*, 1993; Ripmeester, 1976, 1986; Czarnecki *et al.*, 1994*a,b*; Wąsicki *et al.*, 1997; Pająk *et al.*, 1998, 2000, 2002). These transitions were found to be evidently related to the molecular dynamics of the pyridinium cation (Ripmeester, 1986) as well as various anions such as BF_4^- (Czarnecki *et al.*, 1994*b*), ClO_4^- (Czarnecki *et al.*, 1994*a*), ReO_4^- (Wąsicki *et al.*, 1997), IO_4^- (Pająk *et al.*, 1998), FSO_3^- (Pająk *et al.*, 2000) and FCrO_3^- (Pająk *et al.*, 2002). It was established that the number of phase transitions in these pyridinium salts depends entirely on the type and structure of the anions. It was also discovered that ferroelectricity, the most interesting physical property, occurs in the pyridinium complexes in which at least two or more phase transitions take place (Czarnecki *et al.*, 1994*a,b*; Wąsicki *et al.*, 1997; Pająk *et al.*, 1998, 2000, 2002).

The mesophases of pyridinium (Py) tetrafluoroborate, perchlorate, perrhenate, periodate, fluorosulfate and fluorochromate form a new family of ferroelectrics. This family of molecular-ionic ferroelectric crystals can be divided into two subgroups, taking into account the symmetry of their prototype high-temperature phase. A trigonal symmetry was determined for PyBF_4 (Czarnecki *et al.*, 1998), PyClO_4 (Czarnecki *et al.*, 1997) and PyFSO_3 (Pająk *et al.*, 2000) forming the first subgroup, while PyReO_4 (Czarnecki & Małuszyńska, 2000; Małuszyńska *et al.*, 2010), PyIO_4 (Małuszyńska *et al.*, 2003) and PyFCrO_3 (Pająk *et al.*, 2002) crystal-

Table 1

Experimental details.

For all structures: $[\text{C}_5\text{H}_5\text{NH}]^+[\text{ClCrO}_3]^-$, $M_r = 215.56$. Experiments were carried out with Mo $K\alpha$ radiation using an Xcalibur, Atlas, Gemini ultra diffractometer.

	Phase (I)	Phase (II)	Phase (III)	Phase (IV)
Crystal data				
Crystal system, space group	Trigonal, $R\bar{3}m$	Trigonal, $R3m$	Monoclinic, Cm	Monoclinic, Cc
Temperature (K)	355	320	298	120
a, b, c (Å)	9.021 (2), 9.021 (2), 9.369 (4)	8.8349 (12), 8.8349 (12), 9.3960 (16)	7.7193 (7), 8.6842 (7), 6.3139 (5)	7.3539 (3), 8.4985 (3), 12.9706 (6)
α, β, γ (°)	90, 90, 120	90, 90, 120	90, 96.250 (9), 90	90, 95.481 (3), 90
V (Å ³)	660.2 (4)	635.15 (16)	420.74 (6)	806.91 (6)
Z	3	3	2	4
μ (mm ⁻¹)	1.56	1.62	1.63	1.70
Crystal size (mm)	$0.5 \times 0.3 \times 0.3$	$0.70 \times 0.25 \times 0.15$	$0.70 \times 0.25 \times 0.15$	$0.2 \times 0.1 \times 0.08$
Data collection				
Absorption correction	–	Multi-scan	Multi-scan	Multi-scan
$T_{\text{min}}, T_{\text{max}}$	–	0.667, 1.000	0.819, 1.000	0.862, 1.000
No. of measured, independent and observed [$I > 2\sigma(I)$] reflections	1606, 305, 44	1845, 401, 194	2023, 884, 571	5194, 1845, 1718
R_{int}	0.055	0.033	0.023	0.027
Refinement				
$R[F^2 > 2\sigma(F^2)], wR(F^2), S$	0.072, 0.268, 0.75	0.049, 0.115, 0.98	0.037, 0.088, 0.82	0.026, 0.064, 1.05
No. of reflections	305	401	884	1845
No. of parameters	18	22	55	125
No. of restraints	0	1	2	2
H-atom treatment	H-atom parameters constrained	H-atom parameters constrained	H-atom parameters constrained	All H-atom parameters refined
$\Delta\sigma_{\text{max}}$	0.897	0.016	0.071	0.025
$\Delta\rho_{\text{max}}, \Delta\rho_{\text{min}}$ (e Å ⁻³)	0.23, –0.10	0.91, –0.24	0.58, –0.23	0.37, –0.23
Absolute structure	–	Flack (1983)	Flack (1983)	Flack (1983)
Flack parameter	–	0.01 (7)	–0.05 (4)	0.831 (17)

Computer programs: *CrysAlis CCD*, *CrysAlis Pro*, *CrysAlis RED* (Oxford Diffraction, 2010), *SHELXS97*, *SHELXL97* (Sheldrick, 2008).

lizing in the orthorhombic system in the space group $Cmcm$ represent the second subgroup. This dichotomy was explained taking into account the size of the counterion related to the ionic radius of its central atom. Small ions B^{3+} , Cl^{7+} and S^{6+} induce a trigonal symmetry, while larger Re^{7+} or I^{7+} induce an orthorhombic one. In the search for other examples of the ferroelectrics within the pyridinium salts we looked at pyridinium chlorochromate $[\text{C}_5\text{H}_5\text{NH}]^+[\text{ClCrO}_3]^-$ with strongly distorted tetrahedral anion symmetry and as expected with a large electric dipole moment. PyClCrO_3 was studied by DSC, NMR and dielectric methods but not by X-ray diffraction (Pająk *et al.*, 1997). This compound appeared to be the first pyridinium salt revealing as many as three solid–solid phase transitions, which occur at 170, 316 and 346 K. The calculated values of the entropy change point to the order–disorder character of the transitions. Here we present for the first time the symmetry and structure of four phases at 355, 320, 298 and 120 K studied by X-ray single-crystal diffraction, together with new calorimetric and dielectric results. It should be emphasized that until now none of the pyridinium salts belonging to the first subgroup (with the trigonal symmetry of the prototype phase) have been fully structurally characterized in low-temperature phases. This was partially due to the complex ferroelastic domains observed at low temperatures. Therefore, the detailed description of all the phases of PyClCrO_3 together with the classification and description of the phase transitions

can be considered as model studies of this interesting group of pyridinium salts.

2. Experimental

Polycrystalline pyridinium chlorochromate (Aldrich cat.: 19,014-4) was recrystallized twice from water solution and pyridinium chlorochromate single crystals were grown from water solution by slow evaporation at a constant temperature of 300 K. The monocrystalline plate was oriented by X-ray diffraction and its two largest faces were found to be (001) and (00 $\bar{1}$) of phase (III). The dielectric hysteresis loop was measured at a frequency of 50 Hz in the direction perpendicular to the (001) plane using a Diamont–Drenck–Pepinsky bridge [RADIOPAN (MD 2/1)].

Heat-capacity measurements were performed by DSC with thermal analysis (Q 2000) apparatus. The DSC runs were recorded upon heating and cooling polycrystalline samples of weight 8.64 mg at a rate of 10 K min⁻¹. Indium standard was used for temperature and enthalpy calibration, and synthetic sapphire was used for heat-capacity calibration.

Irregularly shaped orange crystals were selected for X-ray diffraction measurements performed at 355, 350, 320, 298 and 120 K with a KUMA-KM4CCD diffractometer equipped with an Oxford Cryostream low-temperature device using Mo $K\alpha$ radiation and the omega scan method. Cell refinement and

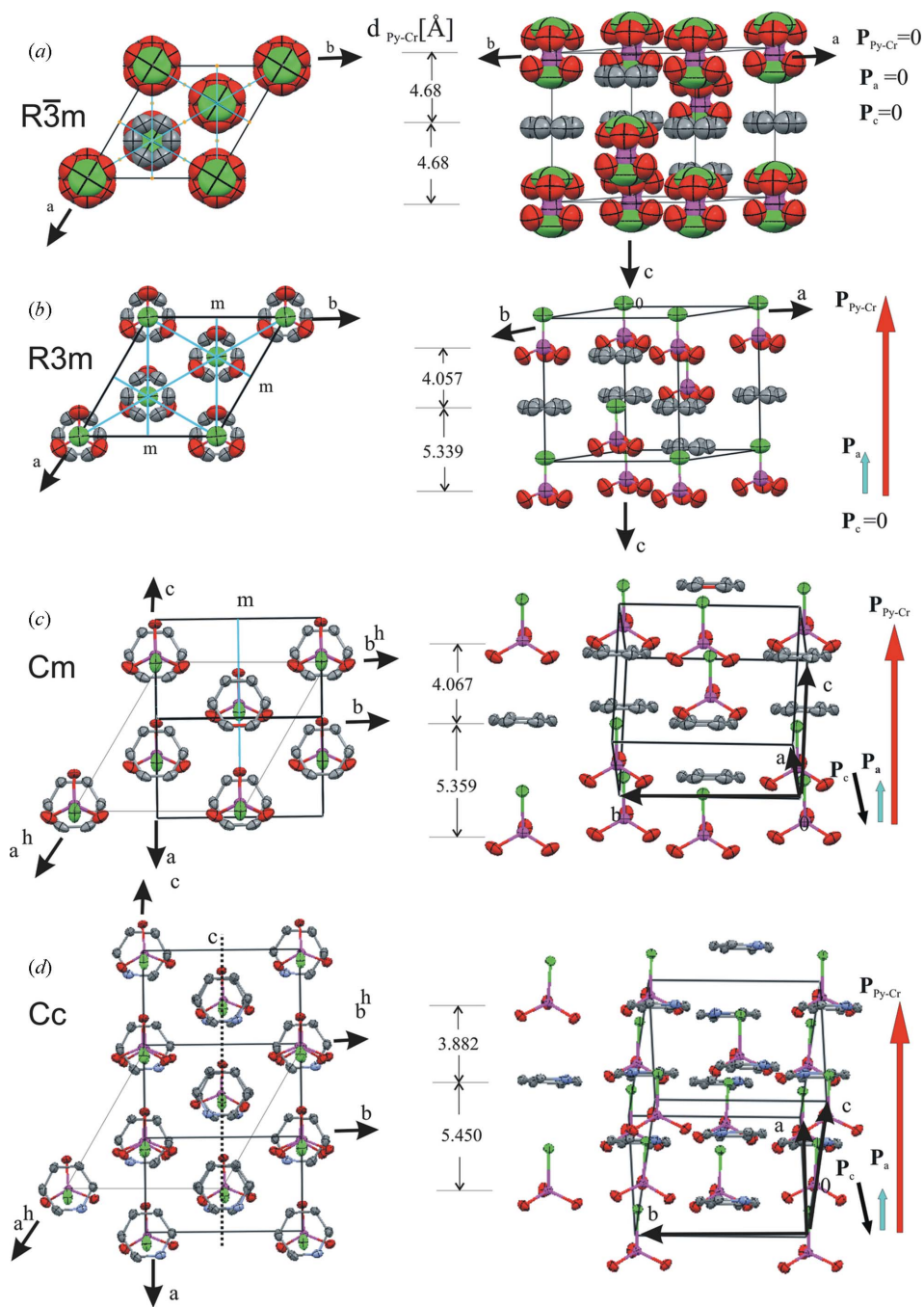


Figure 1 Packing arrangement in four crystal phases; on the left down the c hexagonal axis, on the right perpendicular to it. The arrows on the right represent the components of spontaneous polarization: $P_{\text{py-Cr}}$ – displacive, P_a – ClCrO_3 and P_c – pyridinium. Cl atoms: green; O atoms: red; Cr atoms: pink; C atoms: gray; N atoms: blue. This figure is in colour in the electronic version of this paper.

data reduction were performed using *CrysAlis Pro* software (Oxford Diffraction, 2010). Several attempts have been made to obtain good datasets due to the domain crystal structure of PyClCrO_3 . Additional difficulties occur at high temperatures in which crystals become unstable. The intensity data were corrected for the Lp factor and absorption with the multi-scan procedure (*SCALE3 ABSPACK*; Oxford Diffraction, 2010).

sets of sites related by a center of symmetry located at its gravity center. The NMR studies (Pająk *et al.*, 1997) also revealed in-plane reorientations of the cation in this phase. Therefore, the cationic disorder should be classified as a

The structures were determined by direct methods with *SHELXS97* (Sheldrick, 2008) and refined by least-squares on F^2 with the *SHELXL97* program (Sheldrick, 2008). The crystallographic, experimental and calculation details of PyClCrO_3 at 355, 320, 298 K and 120 K are presented in Table 1.¹

3. Results and discussion

3.1. X-ray measurements

3.1.1. Phase (I) at 355 K. As in all pyridinium salts of the first subgroup, that is in PyBF_4 , PyClO_4 and PyFSO_3 , the high-temperature prototype phase (I) of PyClCrO_3 belongs to the trigonal system with space group $R\bar{3}m$. Its crystal structure is isostructural with the prototype phase of all members of this subgroup. Since the ClCrO_3^- anion is larger than all the other anions creating these pyridinium salts, orthorhombic symmetry with space group $Cmcm$ of the high-temperature prototype phase, rather than trigonal symmetry, was expected. The hexagonal unit comprises three pyridinium cations and three ClCrO_3^- anions. The $mm2$ symmetry of the pyridinium cation and the threefold symmetry of the chlorochromate anion are inconsistent with the $\bar{3}m$ symmetry of the sites occupied by both ions which causes a high orientational disorder of both ions. The pyridinium ion is disordered over six equivalent orientations in the plane perpendicular to the $\bar{3}$ axis and the N atom is equally distributed over six sites of the pyridine ring. The chlorochromate ion with threefold symmetry occupies two

¹ Supplementary data for this paper are available from the IUCr electronic archives (Reference: EB5013). Services for accessing these data are described at the back of the journal.

Table 2
Selected geometric parameters (Å, °).

Phase (I)	Phase (II)		Phase (III)		
Cr1—O	1.52 (2)	Cr1—O1 ⁱ	1.578 (5)	Cr—O2	1.568 (5)
Cr1—Cl ⁱⁱ	1.91 (5)	Cr1—O1	1.578 (5)	Cr—O1	1.593 (3)
C—C ⁱⁱⁱ	1.332 (6)	Cr1—Cl	2.116 (4)	Cr—Cl	2.140 (2)
		C—C ^{iv}	1.334 (10)	C1—C3	1.316 (6)
		C—C ^v	1.326 (11)	C1—C2	1.335 (6)
				C2—C2 ^{vi}	1.336 (10)
				C3—C3 ^{vi}	1.383 (11)
	Phase (IV)				
	Cr—O3		1.598 (2)		
	Cr—O1		1.5984 (16)		
	Cr—O2		1.6209 (16)		
	Cr—Cl		2.1761 (7)		
	N—C5		1.341 (3)		
	N—C1		1.342 (4)		
	C1—C2		1.367 (4)		
	C2—C3		1.380 (4)		
	C3—C4		1.369 (4)		
	C4—C5		1.367 (3)		
	O3—Cr—O1		110.96 (9)		
	O3—Cr—O2		110.60 (9)		
	O1—Cr—O2		111.11 (12)		
	O3—Cr—Cl		108.00 (9)		
	O1—Cr—Cl		108.04 (7)		
	O2—Cr—Cl		107.99 (7)		
	C5—N—C1		122.11 (19)		
	N—C1—C2		119.6 (2)		
	C1—C2—C3		119.2 (2)		
	C4—C3—C2		120.1 (2)		
	C5—C4—C3		119.2 (2)		
	N—C5—C4		119.8 (2)		

Symmetry codes: (i) $-x + y, -x, z$; (ii) $-x, -y, -z$; (iii) $x - y, x, -z + 1$; (iv) $-x + y, y, z$; (v) $-y, -x, z$; (vi) $x, -y, z$.

dynamic one. The character of the disorder of the chlorochromate anion cannot be resolved by X-ray diffraction methods alone since no NMR data are available. Therefore, both static or dynamic disorders remain possible. A model of the static disorder can be characterized by an equal distribution of the chlorochromate anions in two sets of sites related by a center of symmetry. The dynamical disorder of the anion can be considered as the anion jumping over the gravity center, which is located in the crystallographic symmetry center.

Much larger anisotropic displacement parameters (ADPs) of the chlorochromate anion at 355 K than at 350 K indicate that the anion is also dynamically disordered. (The structural results of the X-ray data also measured at 350 K are not included in this paper but are available from the authors.)

The strongly disordered structure and large ADPs in this phase significantly reduce the number of observations in this X-ray structure determination. Therefore, the geometric dimensions of both ions in phase (I), given in Table 2, are not very reliable and cannot be more precisely determined.

The packing arrangement is presented in Fig. 1(a). The pyridinium cation is surrounded by six disordered anions: three lying above and three below the cation plane with the distance between the planes of 1/6 of parameter c . The inter-

Table 3
Selected hydrogen-bond parameters.

$D-H \cdots A$	$D-H$ (Å)	$H \cdots A$ (Å)	$D \cdots A$ (Å)	$D-H \cdots A$ (°)
Phase (II)				
C—H0A \cdots O1 ⁱ	0.96	2.40	3.277 (5)	152.7
Phase (III)				
C3/N—H3A \cdots O1 ⁱⁱ	0.93	2.29	3.155 (6)	155.0
C1—H1A \cdots O2 ⁱⁱⁱ	0.93	2.41	3.250 (4)	149.5
C2—H2A \cdots O1 ^{iv}	0.93	2.54	3.400 (6)	153.8
Phase (IV)				
N—H \cdots O2 ^v	0.97 (3)	1.90 (3)	2.839 (3)	162 (3)
C1—H1 \cdots O3 ^{vi}	0.90 (3)	2.64 (3)	3.014 (3)	106 (2)
C1—H1 \cdots O1 ^{vii}	0.90 (3)	2.57 (3)	3.303 (3)	139 (2)
C2—H2 \cdots O3 ^{viii}	0.98 (3)	2.34 (3)	3.242 (3)	152 (2)
C3—H3 \cdots O1 ^{iv}	0.87 (4)	2.59 (4)	3.330 (3)	143 (3)
C4—H4 \cdots O2 ^{iv}	0.81 (4)	2.71 (4)	3.455 (3)	152 (3)
C5—H5 \cdots O3 ^v	1.00 (3)	2.32 (3)	3.188 (3)	145 (2)

Symmetry code(s): (i) $-x + y - \frac{1}{3}, -x - \frac{2}{3}, z + \frac{1}{3}$; (ii) $x + \frac{1}{2}, -y + \frac{1}{2}, z + 1$; (iii) $x + \frac{1}{2}, y + \frac{1}{2}, z + 1$; (iv) $x + 1, y, z$; (v) $x + \frac{1}{2}, -y - \frac{1}{2}, z + \frac{1}{2}$; (vi) $x, -y, z + \frac{1}{2}$; (vii) $x + \frac{1}{2}, -y + \frac{1}{2}, z + \frac{1}{2}$.

ionic C/N \cdots O distance is 3.44 (2) Å, and the equal distance between the anion above and below the cation is 4.68 (2) Å, see Fig. 1(a).

3.1.2. Phase (II) at 320 K. At 346 K the PyClCrO₃ undergoes a first-order discontinuous phase transition into the non-centrosymmetric polar space group $R3m$. The same space-group symmetry of the mesophase was observed only in pyridinium perchlorate (Czarnecki *et al.*, 1997) and also in ferroelectric imidazolium perchlorate (Pajak *et al.*, 2006). Both ions remain on the threefold axis, but they are no longer located on the center of symmetry. The pyridinium ion is dynamically disordered over six sets of sites, while the chlorochromate ion is ordered but free to undergo reorientations around a threefold crystallographic axis. The dynamic behavior of the pyridinium cation was well observed in the NMR studies reported by Pająk *et al.* (1997). The geometrical dimensions of both ions listed in Table 2 are more precisely determined than in phase (I). The differences between the bond lengths and valency angles in phases (I) and (II) are not significant due to the low precision of their values in phase (I). The environment of the cation in the non-centrosymmetric structure of phase (II) is similar to the environment in the centrosymmetric phase (I), except for the ordering of the chlorochromate anions. The C/N \cdots O distance between the pyridinium cation and the chlorochromate anion become shorter by $\sim 10\%$ and the distances between the gravity centers of the pyridinium and chlorochromate ions become unequal: $d_{\text{py-Cr}} = 5.339$ (10) and 4.057 (10) Å (see Fig. 1b).

3.1.3. Phase (III) at 298 K. At 316 K a second discontinuous phase transition is observed, changing the trigonal system of PyClCrO₃ into a monoclinic one with the space group Cm . The symmetry change from $R3m$ to Cm implies that the phase transition is ferroelastic (Aizu, 1970) and is accompanied with the appearance of ferroelastic domains, also called orientational states. According to Sapriel (1975) three ferroelastic domains can appear within this symmetry change. These orientational states are energetically equivalent, but differ in

their orientations with respect to the prototype structure. They can coexist in one crystal, which becomes a twinned one. The existence of ferroelastic domains in PyClCrO_3 observed with a polarizing microscope results in twinning of the crystals below 316 K and makes the structure determination of phase (III) and especially phase (IV) difficult.

At the phase transition from phase (II) to (III) the threefold axis vanishes and only one of three mirror planes perpendicular to the hexagonal axis a and b in phase (II) remains (see Fig. 1c). The pyridinium cation located on the m mirror plane perpendicular to the monoclinic crystallographic b axis is disordered over two orientations, while the chlorochromate anion also lying on this mirror plane becomes ordered. The N atom of the pyridinium ion was located by inspection of the possible $\text{N}-\text{H}\cdots\text{O}$ hydrogen bonds which are probably responsible for the ordering of the structures in both lower-temperature phases (III) and (IV). The remaining N atom sites were also refined, but gave a slightly higher R factor and longer $\text{C}/\text{N}\cdots\text{O}$ distances. The crystallographic results obtained here confirm the possibility of the in-plane reorientations (but no tumbling nor diffusion) of the cation over two orientations reported in the NMR study (Pająk *et al.*, 1997). They also do not exclude reorientations of the chlorochromate ion around its threefold axis, which in this crystal phase is no longer a crystallographic one, but is tilted by 6.5° in the ac plane. At room temperature the environment of the pyridinium cation becomes less symmetric and the $\text{C}/\text{N}\cdots\text{O}$ distances range from 3.155 (6) to 3.400 (6) Å (Table 3) and $d_{\text{py-Cr}} = 5.359$ (6) and 4.067 (6) Å. The packing diagram of phase (III) is shown in Fig. 1(c).

3.1.4. Phase (IV) at 120 K. At 170 K PyClCrO_3 undergoes a weak second-order phase transition, clearly observed as the C_p anomaly in Fig. 2. The existence of this phase transition was also confirmed by the NMR and dielectric measurements reported by Pająk *et al.* (1997). The second-order/continuous character of this phase transition can be deduced from the shape of the C_p change (see Fig. 2) and from the epsilon changes in the dielectric measurements (see Fig. 5 in Pająk *et*

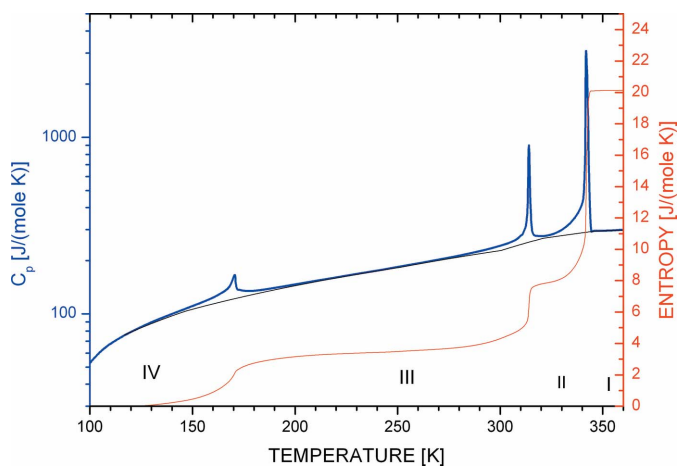


Figure 2
Molar heat capacity C_p and entropy change as a function of molar temperature. Note the logarithmic scale of C_p .

al., 1997). While the existence of this structural phase transition leaves no doubts, the symmetry of phase (IV) is not an easy task to determine and merits deeper consideration.

The diffraction data collected below 170 K on several crystals pointed to Cm symmetry, which is identical to the symmetry of phase (III). This is contrary to the theory of phase transitions which requires that a continuous phase transition must accompany structural and symmetry changes. Additionally the new space group of phase (IV) of PyClCrO_3 should be a subgroup of the space group Cm . The crystal structure of phase (IV) was refined in Cm , Pm and $P1$ space groups (subgroups of the Cm) with very similar results, but the space-group checking routines like ADDSYMM from PLATON (Spek, 2009), which are added to the checkCIF procedure, always pointed to Cm symmetry. Additionally, a careful inspection of the molecular symmetry in Pm and $P1$ also indicated a higher symmetry. As mentioned in §3.1.3, ferroelastic domains are observed in phase (III) and their existence also in phase (IV) could explain the difficulties in determining the correct symmetry of PyClCrO_3 . On the other hand, ferroelastic domains also exist in phase (III) with properly chosen crystal symmetry. Therefore, ferroelastic domains alone could not be responsible for the incorrect symmetry of phase (IV).

The problem of the correct symmetry of phase (IV) was solved with a systematic and careful inspection of the reconstructed precession photographs of the X-ray data collected at 120 K. It turned out that the space group is Cc , a sub-group of Cm , with $c' = 2c$. The reflections with hkl , $l = 1/2, 3/2$ etc., of the Cm space group are several times weaker than the hkl

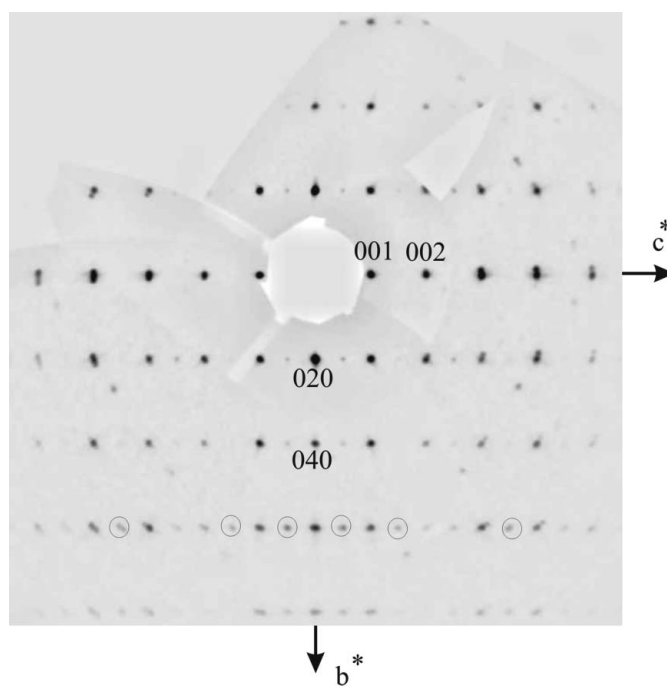


Figure 3
A reconstructed $0kl$ precession image of the Cm monoclinic cell at 120 K. Reflections in circles indicate doubling of the c axis in phase (IV).

reflection with $l = 1, 2, 3$ etc. (see Fig. 3) and were treated as unobserved and ignored by unit-cell finding procedures.

In phase (IV) there are four chlorochromate ions and four pyridinium ions in the unit cell. Both ions are fully ordered and they are both located on the c plane, not on the m mirror plane as in phase (III). The mirror m plane perpendicular to the b axis of the space group Cm of phase (III) becomes a translational c plane in Cc of phase (IV). As a result the pyridinium cation becomes fully ordered and the c parameter doubled. In fact the ordering of the pyridinium cation is responsible for the order-disorder phase transition between phase (III) and (IV). Since the diffraction power of the pyridinium cation is almost twice as low as that of the chlorochromate anion, determination of the correct symmetry of phase (IV) was difficult.

Structure refinement of phase (IV) converged to an R value of 0.026, the lowest of all four phases, see Table 1. The refinement of the absolute structure parameter x (Flack, 1983) to the value of 0.831 (17) indicates some degree of inversion twinning and suggests that the structure may need to be inverted. However, in order to have the two monoclinic structures of phase (III) and (IV) in a consistent coordinate set the absolute structure was not inverted into a second enantiomorph.

The molecular dimensions of both pyridinium and chlorochromate ions, and the intermolecular distances are presented in Tables 2 and 3. They differ significantly from the values observed in phase (III) due to ordering of the pyridinium cation and to ADPs values which are ~ 3 times smaller. The longest Cr–O bond of 1.609 (16) Å of the chlorochromate anion is to the O2 atom involved in the N–H \cdots O hydrogen bond. It is interesting to note that in this phase all the H atoms were localized on the difference-Fourier map and refined isotropically. The relatively small symmetry change between phase (III) and (IV) results not only in ordering of the pyridinium cation, but also in the less symmetric environment of this ion. The N/C \cdots O distances range from 2.839 to 3.455 (3) Å, and $d_{\text{py-Cr}} = 5.450$ (3) and 3.882 (3) Å. The tilt (defined as the angle between the pseudo- C_3 axis of the chlorochromate ion and the c axis of the trigonal system in the hexagonal representation) of the chlorochromate ion in the ac plane is 11.5° [6.5° in phase (III), and 0° in phase (II) and (I)]. The packing diagram of phase (IV) is presented in Fig. 1(d).

3.2. The unit-cell transformation

In order to describe the three phase transitions with respect to one coordinate system the unit-cell dimensions of phase (I) and (II) were transformed into the pseudo-monoclinic C-centered system using the following matrix: $-2/3, -1/3, 2/3; 0, -1, 0; 2/3, 1/3, 1/3$. In this way the unit-cell dimensions of all

Table 4

Unit-cell dimensions (Å, °) of PyClCrO_3 at 355, 320, 298 and 120 K transformed into monoclinic C-centered and rhombohedral systems.

The coordinate system of phase (I) and (II) is a pseudo-monoclinic C-centered representation of phases (II) and (IV) in pseudorhombic systems.

Phase/ T	a_m	b_m	c_m	β_m	a_r	b_r	c_r	$\alpha_r = \beta_r$	γ_r
(I)/355	8.133 (2)	9.021 (2)	6.073 (1)	98.9 (1)	$a_r = b_r = c_r = 6.073$			95.93	95.93
(II)/320	8.078 (2)	8.835 (2)	5.986 (1)	97.61 (1)	$a_r = b_r = c_r = 5.986$			95.12	95.12
(III)/298	7.7193 (7)	8.6842 (6)	6.3139 (5)	96.249 (5)	$a_r = b_r = 5.809$	6.314		94.15	96.73
(IV)/120	7.3539 (3)	8.4985 (3)	12.9706 (6)	95.481 (3)	5.519	5.619	12.971	93.58	98.26

four crystal phases listed in Table 4 are given in the same representation. The unit-cell dimensions in phase (I) and (II) do not change much, while the crystal loses its center of symmetry. The transition from $R3m$ (II) into Cm (III) is connected with the shortening of the a_m and b_m axes of 0.36 and 0.15 Å, respectively, lengthening of the c_m axis of 0.33 Å and decreasing the β_m angle by 1.36°. A similar tendency is observed at the third transformation from Cm (III) into Cc (IV), except the c parameter which becomes doubled.

The cell dimensions of four phases are also listed in the rhombohedral [phase (I) and (II)] and pseudo-rhombohedral cell [phase (III) and (IV)]. The transformation matrix from monoclinic to rhombohedral system is: $1/2, 1/2, 0; 1/2, -1/2, 0; 0, 0, 1$.

4. Calorimetry results and hysteresis loop measurements

The molar heat-capacity measurements (C_p) on the polycrystalline sample in the temperature range 100–360 K are shown in Fig. 2. A similar result was obtained from the measurements on a small single crystal. There are three C_p anomalies at temperatures $T_1 = 343$, $T_2 = 313$ and $T_3 = 170$ K corresponding well to the phase transitions reported earlier (Pająk *et al.*, 1997). The calculated change of entropy associated with the phase transitions is

$$\Delta S = \int_{T_{\min}}^T \frac{C_p - C_b}{T} dT, \quad (1)$$

where C_p is the molar heat capacity obtained by the DSC method, C_b is a baseline (Fig. 2), T and T_{\min} is the temperature range. The results of integration are shown in Fig. 2 on the right-hand scale.

The change of entropy at the phase transition is related to the number of independent orientations of ions in the unit cell, as described by the formula

$$\Delta S = R \ln(n_1/n_2), \quad (2)$$

where R is the gas constant, n_1 and n_2 are the numbers of independent orientations of ions in the crystal phases above and below the phase transition temperature.

These changes in entropy at T_1 , T_2 and T_3 are evidently correlated with the structure of the subsequent phase transitions. The low-temperature phase (IV) with symmetry Cc can

be considered as fully ordered. Phase (III) between temperatures T_3 and T_2 is disordered with two orientations of N atom in the pyridinium cation (Fig. 4a).

According to (2), the change in entropy between phases (IV) and (III) should be $R\ln(2/1) = 5.8 \text{ J mol}^{-1}\text{K}^{-1}$, which is close to the value $\Delta S_1 \simeq 4 \text{ J mol}^{-1}\text{K}^{-1}$ obtained from Fig. 2.

There are six N atom sites of the cation in phase (II) (Fig. 4a). Therefore, the change of entropy between phases (III) and (II) should be $R\ln(6/2) = 9.13 \text{ J mol}^{-1}\text{K}^{-1}$, while the lower value obtained from Fig. 2 is $\Delta S_2 \simeq 4 \text{ J mol}^{-1}\text{K}^{-1}$.

The entropy change between phases (II) and (I) should be $R\ln[(2 \times 6)/6] = 5.8 \text{ J mol}^{-1}\text{K}^{-1}$ because in phase (I) there are two more orientations of the disordered ClCrO_3^- (Fig. 4b). The higher value of $\Delta S_3 \simeq 12 \text{ J mol}^{-1}\text{K}^{-1}$ is obtained from C_P (see Fig. 2). Although there are differences in the estimated entropy changes in the subsequent phase transitions, the summarized entropy change $\Delta S = \Delta S_1 + \Delta S_2 + \Delta S_3 = 20.1 \text{ J mol}^{-1}\text{K}^{-1}$ between temperatures 100 and 360 K is in good agreement with the value obtained from (2). The most disordered is phase (I). The number of independent orientations is equal to the multiplication of the N-atom positions (6) and the positions of anion (2): $n_1 = 2 \times 6 = 12$ (Fig. 4). In the ordered phase (IV) there is only one orientation, $n_2 = 1$ (Fig. 4), and the complete entropy change should be $\Delta S = R\ln(12/1) = 20.7 \text{ J mol}^{-1}\text{K}^{-1}$, which is in good agreement with the value $20.1 \text{ J mol}^{-1}\text{K}^{-1}$ obtained from C_P measurements.

The heat-capacity measurements and entropy change analysis enabled us to conclude that all three phase transitions are of the order–disorder type. The most ordered is phase (IV) and as the temperature rises in subsequent phase transitions the disorder of the ions increases more and more (Fig. 4): the cation disorder at T_3 and T_2 and the anion disorder at temperature T_1 .

A similar entropy analysis at the phase transitions was carried out for PyBF_4 (Hanaya *et al.*, 2000), but the authors only knew the crystalline structure of one phase. Having the crystal structure of four phases of PyClCrO_3 , the above-described entropy analysis gave some correlations between

structural disorder and entropy changes at the phases transitions in this compound.

The hysteresis loop recorded at 310 K is presented in Fig. 5.

The observation of a hysteresis loop is direct evidence proving the ferroelectric character of the material studied. However, it can hardly be used to estimate the maximum polarization. The plates grown permitted measurement only along one direction, providing only one component of polarization.

Knowing the structures of all phases it is possible to describe the nature of ferroelectricity and to estimate approximately the value of polarization in polar phases. Spontaneous polarization results from a nonzero dipole moment of the elementary cell. In this crystal the dipole moment of the elementary cell has two components: the displacive one following from the relative displacement of ions $P_{\text{py-Cr}} = q \times d_{\text{py-Cr}}$ (q = the ion charge) and the orientational component following from the ordering of dipoles of the pyridinium cation (P_c) and ClCrO_3^- anion (P_a).

Of course, in the centrosymmetric phase (I) the spontaneous polarization is zero ($P_s = 0$) because the displacive component resulting from the displacement of the centers of gravity of the ions is zero, $d_{\text{py-Cr}} = (4.684 - 4.684 \text{ \AA})$; Fig. 1a). The orientational component is also zero as the anion undergoes reorientation between two positions and its resultant dipolar moment is zero (Fig. 4b). The pyridinium cation undergoes reorientations between six positions and its mean dipolar moment is also zero (Fig. 4a).

In the ferroelectric phase (II) there are two components of spontaneous polarization: the displacive component resulting from nonzero displacement $d_{\text{py-Cr}} = (5.339 - 4.057 \text{ \AA})$; Fig. 1b), whose contribution to spontaneous polarization is $P_{\text{py-Cr}} = 9.7 \text{ \mu C cm}^{-2}$, and the orientational component resulting from ordering of the anion (Fig. 4b), whose dipole moment is along the threefold axis. Since the reorientation of the pyridinium cation does not change in phase (II) (Fig. 4a), its dipole moment does not contribute to the spontaneous polarization. The calculated dipole moment of ClCrO_3^- with GAUS-

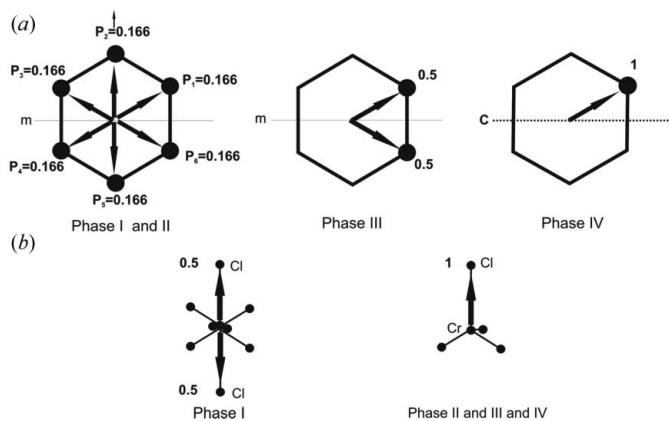


Figure 4 Distribution of (a) the N atoms in the pyridinium cation and (b) the Cl atoms in the ClCrO_3^- anion in four crystal phases. The numbers are the population probability of the N/Cl atoms in the ions. The arrows denote the orientations of the dipole moments.

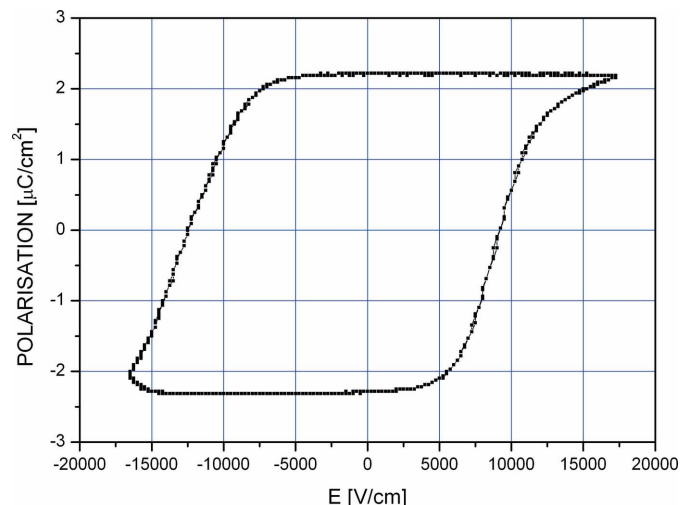


Figure 5 Hysteresis loop recorded at 310 K.

SIAN98 (RHF/CEP-121G set) is 1.37 D in phase (II), which results in the spontaneous polarization of $\sim P_a = 2.19 \mu\text{C cm}^{-2}$ along the threefold axis. The sum of the displacive and orientational polarizations is close to $P_s = P_{\text{py-Cr}} + P_a = 11.9 \mu\text{C cm}^{-2}$. This value is a few times higher than the spontaneous polarization of other ferroelectric pyridinium salts (Czarnecki *et al.*, 1994a; Wąsicki *et al.*, 1997; Pająk *et al.*, 1998, 2000, 2002).

Vujosevic *et al.* (2006) discussed the nature of ferroelectricity in other pyridinium salts and found that for small anions there is antiferroelectric coupling between pyridinium cations. In PyClCrO_3 the anionic and displacive contributions to polarization have the same direction, which excludes their antiferroelectric coupling (see Fig. 1).

In the ferroelectric phase (III) the pyridinium cation is partly ordered (Fig. 4a) and the additional polarization component from its dipole moment ($1.97 \mu\text{C cm}^{-2}$; Małuszyńska *et al.*, 2010) is *ca* $P_c = 2.77 \mu\text{C cm}^{-2}$. Its direction is almost perpendicular to the displacive component $\mathbf{P}_{\text{py-Cr}}$ and to the component from the orientation of the anions, \mathbf{P}_a (Fig. 1c). The vector sum of these components in phase (III) is approximately $\mathbf{P}_s = \mathbf{P}_{\text{py-Cr}} + \mathbf{P}_a + \mathbf{P}_c = 12.2 \mu\text{C cm}^{-2}$ and is located in the mirror plane *m* of the monoclinic system.

In phase (IV) the cations become ordered (Fig. 4a) and the displacement $d_{\text{py-Cr}} = (5.450-3.882 \text{ \AA})$ increases (Fig. 1d). The spontaneous polarization in this phase has three components, $\mathbf{P}_{\text{py-Cr}}$, \mathbf{P}_a and \mathbf{P}_c , and is close to $14.8 \mu\text{C cm}^{-2}$.

In the pyridinium salts studied here, the nature of ferroelectricity is related to the dipole ordering of the pyridinium cations, the ordering of the distorted tetrahedral anion dipoles and the asymmetric displacement of these ions with respect to each other. In the PyBF_4 , PyClO_4 , PyIO_4 and PyReO_4 salts the dipole moment of the distorted tetrahedral anions is small and equal to 0.2–0.3 D (Małuszyńska *et al.*, 2003, 2010; Pająk *et al.*, 2006), while it is close to 1.37 D in PyClCrO_3 with a highly asymmetric anion. The dipole moment of the pyridinium cation is estimated to be 1.97 D (Małuszyńska *et al.*, 2010). The spontaneous polarization in PyClCrO_3 is much greater than in PyIO_4 , PyReO_4 , PyBF_4 or PyClO_4 , because the displacive and orientational components of the distorted tetrahedral ClCrO_3^- anion are increased substantially. PyIO_4 and PyReO_4 were classified according to order–disorder ferroelectrics with a small contribution from the displacive component, while PyClCrO_3 was classified according to mixed displacive and order–disorder ferroelectrics.

5. Conclusions

(i) Pyridinium chlorochromate undergoes three reversible phase transitions with the following sequence of space groups: $R\bar{3}m$ (346 K) $\rightarrow R3m$ (316 K) $\rightarrow Cm$ (170 K) $\rightarrow Cc$, $c' = 2c$.

(ii) All four phases: paraelectric phase (I) at 355 K, ferroelectric (II) at 320 K, ferroelectric (III) at 298 K and most probably ferroelectric phase (IV) at 120 K are fully characterized with single-crystal X-ray diffraction studies. The symmetry and structure of the low-temperature crystal phases

[(III) and (IV)] of pyridinium salts with trigonal symmetry of the prototype phase are reported for the first time.

(iii) The three high-temperature phases (I), (II) and (III) are disordered, from the disorder of both ions in phase (I), the ordered chlorochromate anion and the disordered pyridinium cation in phases (II) and (III). A fully ordered structure characterizes phase (IV). The N–H \cdots O hydrogen bonds seem to be responsible for the ordering of phase (IV) and anion ordering in phases (II) and (III).

(iv) Analysis of the entropy shows a correlation between structural disorder and entropy changes in phase transitions.

(v) All three reversible phase transitions are of the order–disorder type.

(vi) Pyridinium chlorochromate is a new ferroelectric of mixed type: displacive and order–disorder.

(vii) The ClCrO_3^- anion with a strongly distorted tetrahedral symmetry does not influence the geometry of the crystal structures of all the mesophases of this pyridinium salt, but increases the value of spontaneous polarization when comparing with other ferroelectric pyridinium salts.

References

- Aizu, K. (1970). *Phys. Rev. B*, **2**, 754–772.
- Czarnecki, P., Katrusiak, A., Szafraniak, I. & Wąsicki, J. (1998). *Phys. Rev. B*, **57**, 3326–3332.
- Czarnecki, P. & Małuszyńska, H. (2000). *J. Phys. Condens. Matter*, **12**, 4881–4892.
- Czarnecki, P., Nawrocik, W., Pająk, Z. & Wąsicki, J. (1994a). *J. Phys. Condens. Matter*, **6**, 4955–4960.
- Czarnecki, P., Nawrocik, W., Pająk, Z. & Wąsicki, J. (1994b). *Phys. Rev. B*, **49**, 1511–1512.
- Czarnecki, P., Wąsicki, J., Pająk, Z., Goc, R., Małuszyńska, H. & Habryło, S. (1997). *J. Mol. Struct.* **404**, 175–180.
- Flack, H. D. (1983). *Acta Cryst.* **A39**, 876–881.
- Hanaya, M., Ohta, N. & Oguni, M. (1993). *J. Phys. Chem. Solids*, **54**, 263–269.
- Hanaya, M., Shibasaki, H., Oguni, M., Nemoto, T. & Ohashi, Y. (2000). *J. Phys. Chem. Solids*, **61**, 651–657.
- Hartl, H. (1975). *Acta Cryst.* **B31**, 1781–1783.
- Horiuchi, S., Ishii, F., Kumai, R., Okimoto, Y., Tachibana, H., Nagaosa, N. & Tokura, Y. (2005). *Nat. Mater.* **4**, 163–166.
- Horiuchi, S., Tokunaga, Y., Giovannetti, G., Picozzi, S., Itoh, H., Shimano, R., Kumai, R. & Tokura, Y. (2010). *Nature*, **463**, 789–792.
- Małuszyńska, H., Cousson, A. & Czarnecki, P. (2010). *J. Phys. Condens. Matter*, **22**, 235901.
- Małuszyńska, H., Scherf, C., Czarnecki, P. & Cousson, A. (2003). *J. Phys. Condens. Matter*, **15**, 5663–5674.
- Oxford Diffraction (2010). *CrysAlis PRO*. Oxford Diffraction Ltd, Yarnton, Oxfordshire, England.
- Pająk, Z., Czarnecki, P., Małuszyńska, H., Szafranska, B. & Szafran, M. (2000). *J. Chem. Phys.* **113**, 848–853.
- Pająk, Z., Czarnecki, P., Szafranska, B., Małuszyńska, H. & Fojud, Z. (2006). *J. Chem. Phys.* **124**, 144502.
- Pająk, Z., Czarnecki, P., Wąsicki, J. & Nawrocik, W. (1998). *J. Chem. Phys.* **109**, 6420–6423.
- Pająk, Z., Małuszyńska, H., Szafranska, B. & Czarnecki, P. (2002). *J. Chem. Phys.* **117**, 5303–5310.
- Pająk, Z., Szafranska, B., Czarnecki, P., Mayer, J. & Kozak, A. (1997). *Chem. Phys. Lett.* **274**, 106–111.
- Ripmeester, J. A. (1976). *Can. J. Chem.* **54**, 3453–3457.

Ripmeester, J. A. (1986). *J. Chem. Phys.* **85**, 747–750.
Sapriel, J. (1975). *Phys. Rev. B*, **12**, 5128–5140.
Sheldrick, G. M. (2008). *Acta Cryst. A* **64**, 112–122.
Spek, A. L. (2009). *Acta Cryst. D* **65**, 148–155.

Vujosevic, D., Müller, K. & Roduner, E. (2006). *J. Phys. Chem. B*, **110**, 8598–8605.
Wąsicki, J., Czarnecki, P., Pająk, Z., Nawrocik, W. & Szczepański, W. (1997). *J. Chem. Phys.* **107**, 576–579.